



Pharmaceutics, Drug Delivery and Pharmaceutical Technology

## Spray Drying as a Reliable Route to Produce Metastable Carbamazepine Form IV



Rebecca A. Halliwell<sup>1</sup>, Rajni M. Bhardwaj<sup>1</sup>, Cameron J. Brown<sup>1,\*</sup>, Naomi E.B. Briggs<sup>1</sup>, Jaclyn Dunn<sup>2</sup>, John Robertson<sup>1</sup>, Alison Nordon<sup>2</sup>, Alastair J. Florence<sup>1</sup>

<sup>1</sup> EPSRC Centre for Innovative Manufacturing in Continuous Manufacturing and Crystallisation, c/o Strathclyde Institute of Pharmacy and Biomedical Sciences, University of Strathclyde, Technology and Innovation Centre, 99 George Street, Glasgow G1 1RD, UK

<sup>2</sup> Pure and Applied Chemistry, University of Strathclyde, Glasgow, UK

### ARTICLE INFO

#### Article history:

Received 9 December 2016

Revised 16 March 2017

Accepted 27 March 2017

Available online 19 April 2017

#### Keywords:

spray drying  
continuous processing  
carbamazepine  
metastable form  
polymorphism  
PAT

### ABSTRACT

Carbamazepine (CBZ) is an active pharmaceutical ingredient used in the treatment of epilepsy that can form at least 5 polymorphic forms. Metastable form IV was originally discovered from crystallization with polymer additives; however, it has not been observed from subsequent solvent-only crystallization efforts. This work reports the reproducible formation of phase pure crystalline form IV by spray drying of methanolic CBZ solution. Characterization of the material was carried out using diffraction, scanning electron microscopy, and differential scanning calorimetry. *In situ* Raman spectroscopy was used to monitor the spray-dried product during the spray drying process. This work demonstrates that spray drying provides a robust method for the production of form IV CBZ, and the combination of high supersaturation and rapid solid isolation from solution overcomes the apparent limitation of more traditional solution crystallization approaches to produce metastable crystalline forms.

© 2017 The Authors. Published by Elsevier Inc. on behalf of the American Pharmacists Association®. This is an open access article under the CC BY license (<http://creativecommons.org/licenses/by/4.0/>).

### Introduction

Active pharmaceutical ingredients (APIs) and formulated dosage forms are largely produced using traditional batch manufacturing methods. However, there is increasing interest in exploiting the potential advantages of continuous processing that include improved consistency, process efficiency, and reduced cost of goods in the manufacture of pharmaceuticals.<sup>1</sup> Spray drying enables particle formation and isolation in a single continuous operation and so presents the opportunity to simplify multiple batch operations into a single step. The present study, therefore, investigates particle formation of the API carbamazepine (CBZ) in a spray dryer.

Many APIs exhibit multiple polymorphic forms that can display different physical attributes.<sup>2</sup> This range of accessible properties can lead to variability during processing and ultimately in use through changes in stability, flow, shape, aerodynamic performance, solubility, dissolution, or bioavailability.<sup>3</sup> Consequently,

there is a requirement to understand and control the polymorphic forms that are used in products. Although capabilities for *ab initio* crystal structure prediction of polymorphs from molecular structure have developed considerably in recent years,<sup>4</sup> they not yet routinely applicable to gain the complexity of typical APIs. Therefore, extensive experimental investigations are still largely required to define the range of potential polymorphic structures, their relative thermodynamic experimental stabilities, and the conditions under which they can be formed.<sup>5</sup>

CBZ is an API which is used in the treatment of epilepsy and trigeminal neuralgia.<sup>6,7</sup> CBZ has a low water solubility (<200 µg/mL)<sup>6</sup> and falls within class II of the Biopharmaceutical Classification System and can show dissolution-limited absorption.<sup>8</sup> The solid-state forms of CBZ have been widely studied, and it has been reported in 5 different polymorphic forms, CBZ I, II, III, IV,<sup>9</sup> and V<sup>10</sup> in addition to a large number of solvated,<sup>11</sup> co-crystalline forms,<sup>12,13</sup> salts,<sup>14</sup> and nanocrystalline forms.<sup>15</sup> The thermodynamically stable form at room temperature is the monoclinic CBZ III.<sup>16</sup>

Polymorphism of CBZ has been widely investigated using different screening approaches,<sup>16,17</sup> theoretical analysis,<sup>18</sup> and crystal structure prediction.<sup>12</sup> CBZ IV was first obtained by re-crystallization from methanol solution in the presence of hydroxypropylcellulose<sup>9</sup> and was subsequently reported using polymer

This article contains supplementary material available from the authors by request or via the Internet at <http://dx.doi.org/10.1016/j.xphs.2017.03.045>.

\* Correspondence to: Cameron J. Brown (Telephone/Fax: +44 (0)141 444 7122).

E-mail address: [cameron.brown.100@strath.ac.uk](mailto:cameron.brown.100@strath.ac.uk) (C.J. Brown).

<http://dx.doi.org/10.1016/j.xphs.2017.03.045>

0022-3549/© 2017 The Authors. Published by Elsevier Inc. on behalf of the American Pharmacists Association®. This is an open access article under the CC BY license (<http://creativecommons.org/licenses/by/4.0/>).

heteronucleation.<sup>19</sup> However, subsequent attempts to obtain form IV from solution, including multiple solvent screens<sup>12</sup> and single solvent screens,<sup>16</sup> did not produce any evidence of CBZ IV. This was explained due to the absence of polymer additives in these studies. Notably, Kiporous et al.<sup>20,21</sup> in a study of analytical techniques for polymorphic mixtures stated CBZ IV used in that study was produced by spray drying from methanol. No further detail on the method was provided or mechanism proposed for the occurrence of CBZ IV.

Spray drying is an important technique for pharmaceutical manufacturing and is generally used to isolate from a suspension through conversion of a liquid or solution stream into a solid powder through controlled, rapid evaporation of solvent or liquid by a heated drying gas.<sup>22</sup> It is well known for the formation of amorphous solids in pharmaceuticals and food areas<sup>23</sup> and being applied to a range of particle engineering applications.<sup>24,25</sup> However, it has also been demonstrated for the production of crystalline particles, such as spray drying of the API salbutamol sulfate,<sup>26</sup> excipient mannitol crystals,<sup>27</sup> and co-crystals of CBZ and nicotinamide.<sup>28</sup>

The present study seeks to investigate the formation of form IV CBZ during spray drying and the potential of polymorph control.<sup>25</sup> Here we report a robust and reproducible method for production of CBZ IV that does not require polymer additives. The application of *in situ* Raman monitoring is also demonstrated.

## Materials and Methods

### Materials

CBZ III was sourced from Molekula and methanol (high-performance liquid chromatography grade,  $\geq 99.5\%$ ) from Sigma-Aldrich.

### Spray Drying Method

CBZ solutions were spray dried using a Büchi B-290 Mini Spray Dryer coupled with the Büchi Inert Loop B-295 (Büchi Labor-technik AG, Flawil, Switzerland) and configured with a high-performance cyclone. The dryer was operated in co-current closed mode with nitrogen as the drying gas. The starting composition of solutions to be introduced into the dryer was 10.4 g/L CBZ in methanol at room temperature. The spray dryer parameters used to obtain a dry powder were aspirator rate 100%, inlet temperature = 393.15 K, outlet temperature = 338.15–348.15 K, pump percentage = 10%, spray gas = 7 bar pressure, and spray gas rate operated between 439 and 667 L/h (at standard temperature and pressure).

### X-Ray Powder Diffraction

All spray-dried powders were analyzed using X-ray powder diffraction (XRPD). Samples were analyzed using transmission foil XRPD data collected on a Bruker AXS D8-Advance transmission diffractometer equipped with  $\theta/\theta$  geometry, primary monochromated radiation (Cu  $K\alpha_1$ ,  $\lambda = 1.54056 \text{ \AA}$ ), a Vantec 1D position-sensitive detector, and an automated sample stage.<sup>29</sup> Samples were mounted on a 28 position sample plate supported on a polyimide (Kapton, 7.5  $\mu\text{m}$  thickness) film. Data were collected from each sample in the range  $4\text{--}35^\circ 2\theta$  with a  $0.015^\circ 2\theta$  step size and 1 s/step count time. Samples were oscillated 0.5 mm in the  $x\text{--}y$  plane at a speed of 0.3 mm/s throughout data collection. Resultant CBZ form was identified by standard procedures including pattern matching and Pawley<sup>30</sup> refinement.

### Scanning Electron Microscopy

The morphology and particle size of spray-dried samples were imaged using a Hitachi SU6600 Analytical VP FEG-SEM. Samples were mounted and analyzed at 5 kV.

### Particle Sizing

Particle size and particle size distributions of the spray-dried samples were analyzed using a Malvern Morphologi G3 instrument. This technique integrates compressed air dispersion with automated microscopy to image and collect size and shape data for the sample particle population. The 3-dimensional particles are imaged in 2 dimensions. The diameter of a circle is then calculated with equal area to the projected area of the particle known as the circle equivalent (CE) diameter.<sup>31</sup>

### Thermal Analysis

Differential scanning calorimetry (DSC) of samples was carried out in a Netzsch STA 449 C instrument. Samples were placed in a 10- $\mu\text{L}$  Al crucible with pierced lid to allow loss of water vapor. The samples were analyzed using a heating rate of 10 K/min from 293.15 to 493.15 K.

### Raman

Raman spectra were also collected from samples using offline measurements and from the spray drier using a Kaiser RXN1 Raman spectrometer equipped with PhAT probe. The PhAT probe uses a class 3 laser beam with a 6-mm spot size and enables noninvasive measurement of Raman spectra from solids.<sup>32</sup> For the offline measurement, a glass vial containing sample was analyzed. For the online measurement, the PhAT probe was positioned at the collection vessel of the high-performance cyclone to measure the final dried product emerging from the process.

## Results and Discussion

### CBZ IV

The spray drying process conditions successfully produced a dry, crystalline CBZ sample. The sample was identified as CBZ IV by comparison of the experimental XRPD data with calculated XRPD reference patterns for forms I-IV (Fig. 1). The data comprised sharp diffraction peaks with no evidence of an elevated background scattering that might indicate amorphous content. This result was confirmed through analysis using a Pawley-type fit<sup>30</sup> (Fig. 2).

The Pawley-type fit to the data from the spray-dried sample was carried out in the TOPAS software package.<sup>33</sup> The fit to the data is very good, and the refined, room temperature lattice parameters obtained were  $a = 26.432(2)\text{ \AA}$ ,  $b = 7.0360(6)\text{ \AA}$ ,  $c = 13.9044(16)\text{ \AA}$ , and  $\beta = 109.570(7)^\circ$ , space group C2/c (cf. the reported values from the single crystal study  $a = 26.609(4)$ ,  $b = 6.927(1)$ ,  $c = 13.957(2)$ , and  $\beta = 109.7(1)^\circ$ , CSD REFCODE: CBMZPN12).<sup>9</sup> There is no evidence of any diffraction peaks from the sample that are not accurately described by the structure of CBZ IV, confirming the phase purity, to the limit of detection for XRPD, of the spray-dried sample.<sup>20,21</sup>

To understand process robustness of the spray dryer with respect to CBZ IV formation, 3 process parameters were varied, specifically, inlet temperature and feed pump rate (conditions 1–3) and solvent (condition 4; Table 1). Conditions were selected that may be expected to effect the rate of drying and initial nucleation conditions within the range required to obtain a dry powder.

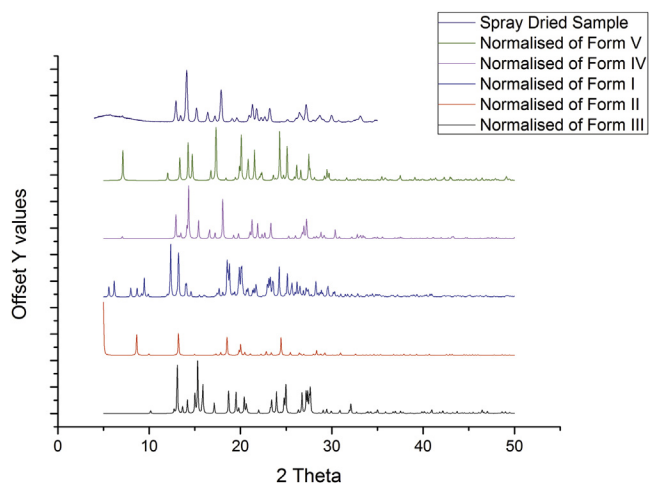


**Figure 1.** Calculated XRPD patterns for CBZ I, II, III, and IV compared with the experimental data for spray-dried methanol CBZ solution.

Noninvasive *in situ* Raman spectroscopy was used to obtain real-time measurements during each of the experiments. To investigate the impact of the different parameters, a comparison of the resultant Raman spectra along with an offline reference of CBZ IV is shown in Figure 3.

The spectra collected from the spray-dried samples produced from each conditions 1–4 (Table 1) show some differences in baseline and signal-to-noise; however, the characteristic Raman bands show a direct correspondence with the form IV Raman reference spectrum. No peaks from alternative CBZ forms were observed. The formation of CBZ IV by spray drying is highly reproducible and relatively insensitive to limited changes in the process conditions and a change of solvent from methanol to ethanol.

Samples of spray-dried CBZ IV were characterized using scanning electron microscopy (SEM) (Fig. 4), particle sizing (Fig. 5), and DSC (Supplementary Data). SEM shows particles with diameters in the between <1 and 5 microns consistent with expectation from the Büchi mini dryer.<sup>34</sup> The particles are reasonably isometric and show clearly defined facets with some evidence of agglomeration. In contrast, Lang et al.<sup>9</sup> reported the morphology of form IV crystals to be “plate like.”

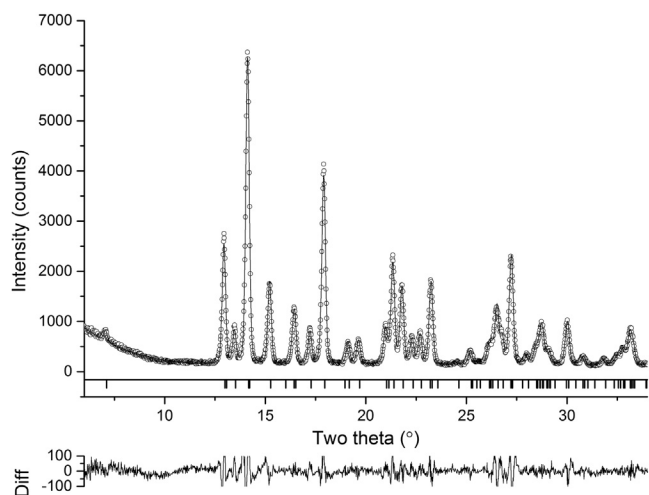


**Figure 2.** Pawley fit of the data from the spray-dried CBZ sample. Observed profile (o), calculated profile (—), and difference plot ( $Y_{obs} - Y_{cal}$ ) of the Pawley fit in the range of 6–34° 2 $\theta$  (weighted profile R-factor = 6.68).

**Table 1**  
Summary of Spray Dryer Conditions Tested

Variable	Inlet Temperature (K)	Pump Rate (%)	Solvent
Original spray drying parameters	393.15	10	Methanol
Condition 1	373.15	10	Methanol
Condition 2	393.15	5	Methanol
Condition 3	373.15	5	Methanol
Condition 4	393.15	10	Ethanol

Particle size and size distribution of spray-dried material were measured using a Malvern Morphologi G3. CE diameter, aspect ratio, and high sensitivity circularity were determined against the volume distribution (Fig. 5).

The CE diameter illustrates a multimodal distribution of particle sizes with a mean size of 5.5  $\mu\text{m}$  with evidence of large aggregates, which is supported by the SEM images.

DSC analysis of the spray-dried samples confirms the expected thermal behavior of CBZ IV (see Supplementary Data) and show good correspondence to the previously reported thermal analysis of anhydrous CBZ polymorphs.<sup>19</sup> Spray-dried samples were shown by XRPD to be stable for at least 3 months at 293.15 K (see Supplementary Data).

#### CBZ IV Solution-Mediated Transformation

Although spray drying of methanol and ethanol CBZ solutions yields form IV, previous crystallization studies that have included recrystallization from methanol solution have not reproduced this metastable form.<sup>9,12,16,19</sup> This is despite the inclusion of conditions conducive to rapid precipitation that may be expected to favor metastable forms.

The original report of CBZ IV<sup>19</sup> produced the polymorph by slow evaporative recrystallization from methanol solution in the presence of hydroxypropylcellulose at room temperature. Getsoian et al.<sup>16</sup> investigated CBZ polymorphs using a single-solvent screen and observed CBZ I, II, and III through temperature and supersaturation control. However, attempts to obtain reference samples of form IV by recrystallization directly from solution were unsuccessful, and a sample was ultimately obtained by de-solvation of a solvated form. It has been concluded that<sup>12</sup> proposed form IV requires polymers to act as templates and their absence prevents crystallization of CBZ IV directly from solution. Electro spray crystallization from methanol solution produced amorphous nanoparticles that transformed to CBZ III or I depending on post-solidification annealing conditions.<sup>35</sup> This suggests under the conditions used in electro spray, solidification occurs so rapidly that nucleation of crystals is predicted.

The reported inconsistency of solution crystallization studies to reproduce CBZ IV is notable. This could indicate that form IV does not nucleate directly from solution and requires the presence of an additive that either templates CBZ IV or inhibits the nucleation of competing forms. However, the occurrence of CBZ IV from spray drying of CBZ solution does not support this conclusion. The relative thermodynamic stabilities of CBZ I, II, III, and IV have been reported as III > I > IV > II based on thermal analysis.<sup>19</sup> Thus, under solution conditions where CBZ IV is nucleated, the metastable form would be expected to transform to the more stable polymorphs CBZ I or III through solution-mediated transformation.<sup>36</sup> It is, therefore, proposed in the spray dryer that the combination of a high rate of supersaturation from rapid evaporation at elevated temperature promotes the formation of metastable CBZ IV and the rapid isolation of the metastable polymorph prohibits subsequent solution-mediated transformation, enabling recovery of solid CBZ IV.

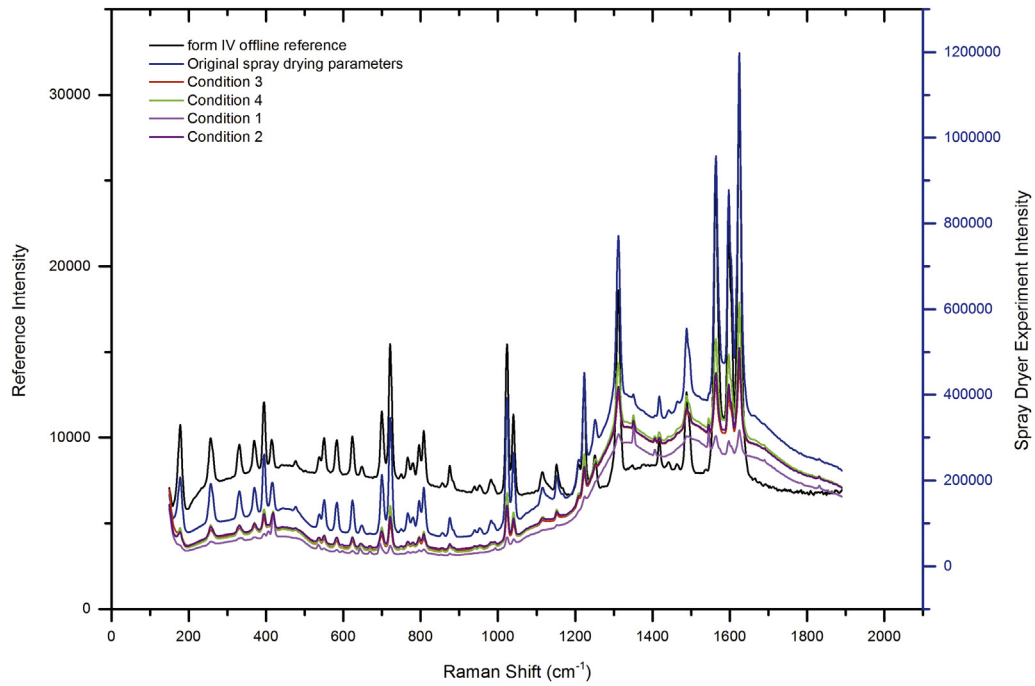


Figure 3. Raman spectra for CBZ samples produced under different spray dryer process conditions and a CBZ IV offline reference.

To support this hypothesis, the diffusion coefficient and drying rates that are crucial in the formation of CBZ IV by spray drying were calculated (Eqs. 1-11), with values for each term given in Table 2. During droplet drying, the diffusivity of CBZ in methanol,  $D_{CBZ/Me}$ , will not only influence the morphology and structure of the final particles but influence the nucleation and growth rates during drying.<sup>35</sup> Throughout the drying process, it was assumed that the droplet liquid was at its wet bulb temperature,  $T_{wb}$ .<sup>37</sup> For drying in  $N_2$  or air, the wet bulb temperature can be estimated from<sup>25</sup>:

$$T_{wb} = 137 \left( \frac{T_b}{373.15} \right)^{0.68} \log(T_G) - 45 \quad (1)$$

$D_{CBZ/Me}$  was calculated to be  $1.101 \times 10^{-9} \text{ m}^2/\text{s}$  using the Wilke–Chang equation.<sup>38,39</sup> Physical properties (viscosity, density, etc.) of the droplet liquid were taken at  $T_{wb}$ .

$$D_{CBZ/Me} = \frac{1.173 \times 10^{-16} \phi_{Me}^{0.5} M_{Me}^{0.5} T}{\mu V_{CBZ}^{0.6}} \quad (2)$$

To estimate the evaporation rate,  $\kappa$ , of methanol from the droplets during drying, using (Eq. 3)<sup>25</sup>

$$\kappa = 8D_{Me/N_2} \frac{\rho_g}{\rho_l} (Y_{S,Me}(T_e) - Y_{\infty,Me}). \quad (3)$$

To calculate  $Y_{S,Me}(T_e)$ , the equilibrium temperature,  $T_e$ , was approximated to the wet bulb temperature,  $T_{wb}$  (Eq. 1). The saturated vapor pressure at this temperature was calculated via the Antoine equation<sup>40</sup> to be 0.060 bar. Furthermore, to estimate the mass fraction of methanol at the surface,  $Y_{S,Me}(T_e)$ , the mole fraction was first calculated from Dalton's law (4) before conversion to a mass fraction:

$$Y_{Me} = \frac{P_{Me}}{P_T} \quad (4)$$



Figure 4. SEM images of spray-dried CBZ IV.

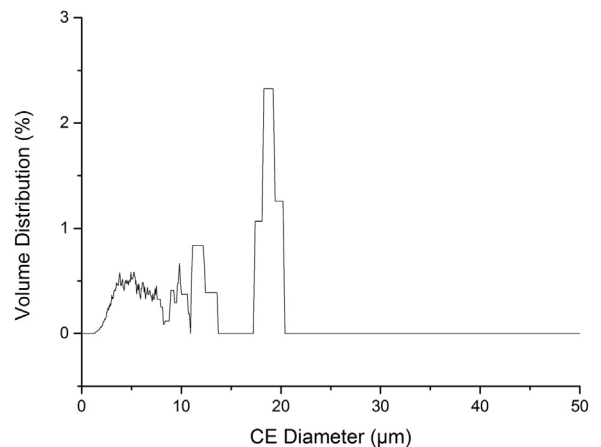


Figure 5. Particle size and size distribution measurements of form IV: CE diameter.

**Table 2**  
Diffusion Coefficient, Evaporation Rate, and Peclet Number Calculation Values

Parameter	Value	Unit
Methanol boiling point, $T_b$	337.85	K
Gas outlet temperature, $T_G$	343.15	K
Wet bulb temperature, $T_{wb}$	279.66	K
Association factor, $\phi$	1.9 <sup>38</sup>	
Molar volume, $V_{CBZ}$	0.155 <sup>42</sup>	m <sup>3</sup> /kmol
Solvent viscosity, $\mu$	$7.11 \times 10^{-4}$ . <sup>43</sup>	N.s/m <sup>2</sup>
Solvent molecular weight, $M_{Me}$	32.04	kg/kmol
Droplet temperature, $T$	279.66	K
Diffusion coefficient, $D_{CBZ/Me}$	$1.101 \times 10^{-9}$	m <sup>2</sup> /s
Diffusion coefficient, $D_{Me/N_2}$	$1.10 \times 10^{-5}$	m <sup>2</sup> /s
Drying gas density, $\rho_g$	1.251	kg/m <sup>3</sup>
Droplet liquid density, $\rho_l$	803.8	kg/m <sup>3</sup>
Mass fraction of solvent away from droplet surface, $Y_{s,Me}$	0	
Methanol saturated vapor pressure, $P_{Me}$	0.060 <sup>40</sup>	bar
Drying chamber pressure, $P_T$	0.91	bar
Mole fraction methanol at droplet surface, $Y_{Me}$	0.066	
Mass fraction methanol at droplet surface, $Y_{S,Me}(T_e)$	0.075	
Evaporation rate, $\kappa$	$1.024 \times 10^{-8}$	m <sup>2</sup> /s
Peclet number, Pe	1.19	
Surface enrichment, $E_{CBZ}$	1.254	
Droplet diameter, $d_0$	25 <sup>34</sup>	$\mu\text{m}$
Drying time, $\tau_D$	0.061	s
Solute initial concentration, $C_0$	0.0104	g/mL <sub>Me</sub>
Saturated concentration, $C_{sol}$	0.0460 <sup>44</sup>	g/mL <sub>Me</sub>
Initial supersaturation, $S_0$	0.226	
Time to crystallization window, $\tau_{sat}$	0.0347	s
Solute true density, $\rho_t$	1.296	g/mL
Initial density, $P_0$	0.008	
Time to amorphous concentration, $\tau_t$	0.0582	s

Therefore, on calculation of Equation 3, the evaporation rate of methanol during drying is estimated to be  $1.024 \times 10^{-8}$  m<sup>2</sup>/s.

The calculated diffusion coefficient of CBZ and the evaporation rate can be expressed by the dimensionless Peclet number, Pe, that calculates the ratio of solvent evaporation to molecular diffusion.<sup>41</sup> If the drying process has a Pe < 1, then the diffusion of the solute is faster than the evaporation rate of the solvent meaning the solute will diffuse to the core of the droplet and create a solid particle. If the drying process has a Pe  $\gg$  1, then the diffusion of the solute is slower than the evaporation of the solvent resulting in shell formation due to enrichment of the solute at the surface of the droplet creating a hollow particle. For CBZ, the Pe number was calculated (Eq. 5)<sup>25</sup>:

$$Pe = \frac{\kappa}{8D_{CBZ/Me}} \quad (5)$$

To further investigate the possible structural outcome of the spray-dried CBZ particles, the level of surface enrichment can be approximated (Eq. 6),<sup>25</sup>

$$E_{CBZ} = 1 + \frac{Pe}{5} + \frac{Pe^2}{100} - \frac{Pe^3}{4000} \quad (6)$$

This equation will indicate the concentration of CBZ at the surface relative to the average concentration of the particle which would equate to 1.

To determine the process times for spray drying of CBZ, the total drying time was calculated (Eq. 7)<sup>25</sup>:

$$\tau_D = \frac{d_0^2}{\kappa} \quad (7)$$

Of the total drying time, a portion of time is required for the concentration to reach the point crystallization can occur,  $\tau_{sat}$ . First, the initial supersaturation,  $S_0$ , can be determined as a ratio of the

initial concentration to the saturated concentration of CBZ in methanol (Eq. 8)<sup>25</sup>:

$$S_0 = \frac{C_0}{C_{sol}} \quad (8)$$

This value can be used to calculate the time during drying after which crystallization of CBZ can be possible (Eq. 9)<sup>25</sup>

$$\tau_{sat} = \tau_D \left(1 - (S_0 E_{CBZ})^{2/3}\right) \quad (9)$$

It is also important to determine the time in which the process would need to gain an amorphous form. First, the initial density of CBZ was determined (Eq. 10)<sup>25</sup>:

$$P_0 = \frac{C_0}{\rho_t} \quad (10)$$

Thus, the time required to produce an amorphous solid (Eq. 11).<sup>25</sup>

$$\tau_t = \tau_D \left(1 - (P_0 \cdot E_{CBZ})^{2/3}\right) \quad (11)$$

As listed in Table 2, the Pe number calculated from Equation 5 was found to be 1.19. This value of approximately 1 suggests that CBZ diffuses into the core of the droplet at almost the same rate that methanol is evaporating. Therefore, an approximately even distribution of CBZ and a solid particle structure would be expected from the process. Furthermore, the surface enrichment of CBZ,  $E_{CBZ}$ , was found to be 1.254, which shows a low level of surface enrichment. Given this low value of surface enrichment and the errors associated with the approximations used in its calculation, it is reasonable to assume that minimal surface enrichment occurs leading to a low likelihood of producing a hollow shell particle. This is backed up by the SEM images in Figure 4, which show isometric and nonspherical-shaped crystalline particles from the spray drying process.

Based on the drying rate as calculated earlier, Figure 6 shows the calculated droplet diameter and CBZ supersaturation within the droplet throughout the constant rate drying period. This period was found to be 0.061 s, and this is realistic compared with the approximated drying residence time of the Büchi of 1–1.5 s.<sup>34</sup> Of this total drying period, the first 0.0347 s is concerned with the evaporation of methanol leading to an increase in CBZ concentration to a supersaturation of 1. After 0.0347 s, crystallization is feasible but may or may not occur depending on the nucleation

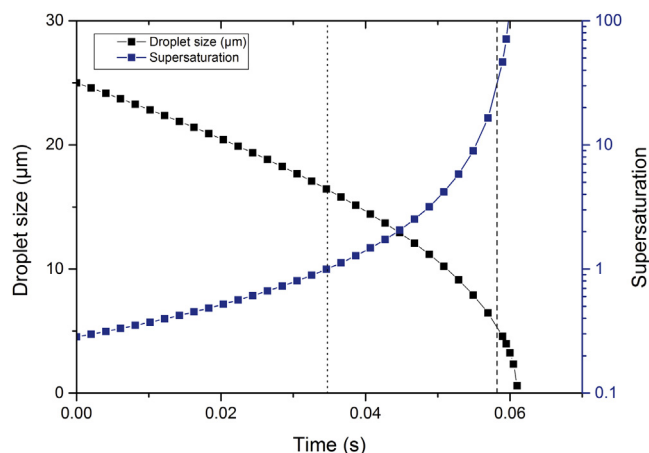


**Figure 6.** Droplet diameter and CBZ supersaturation as a function of drying time.

kinetics. Furthermore, at 0.0582 s if crystallization has not occurred, the concentration of CBZ will be equal to the true density of solid CBZ. After this point, an amorphous material can be expected. When comparing the time to reach the true density with the supersaturation curve in Figure 6, the maximum supersaturation before amorphous formation was found to be  $S = 34.59$ . As the XRPD patterns shown in Figure 1 do not provide any evidence of the presence of amorphous material, it can be assumed that CBZ crystallized before this time and supersaturation was reached. Therefore, it can be concluded that the nucleation kinetics of CBZ are such that spontaneous nucleation of CBZ IV occurs between supersaturations of 1 and 34.59.

The final step in the formation of CBZ IV is the consideration of solution-mediated transformation. O'Mahony et al.<sup>36</sup> describe the solution-mediated transformation of CBZ I–III on the scale of minutes. Based on the previously calculated process times if CBZ IV nucleated at a supersaturation of 1, particles would only be in contact with solvent for a further 0.0263 s by which all the solvent was removed through drying. Therefore, in comparison with the times detailed,<sup>36</sup> solution-mediated transformation to a more stable form may be unlikely.

To further investigate this supersaturation, evaporation rate and particle isolation were studied independently out with the dryer. First in terms of supersaturation, the high inlet temperature used in the spray dryer will lead to rapid evaporation of solvent from the surface of the droplets and a rapid rise in supersaturation until primary nucleation of CBZ occurs. Under high supersaturations, metastable polymorphs are more likely.<sup>16</sup> However, due to the multiple spray dryer conditions that contribute to supersaturation, such as feed concentration, drying temperature, drying rate, droplet diameter, and number, experimental measurement of supersaturation in droplets during the process may be unfeasible. In an attempt to replicate the spray dryer conditions to study supersaturation, rapid cooling of methanol solutions from 328.15 to 263.15 K of 5 mL was performed in a multi-position crystallization platform. Samples were monitored for the onset of crystallization and crystalline samples quickly removed, dried, and analyzed to identify polymorphic form using XRPD (Fig. 7).

All recrystallized CBZ samples were confirmed as the stable CBZ III form. Getsoian et al.<sup>16</sup> suggest that form II is more likely to be produced under high supersaturation; however, Sypek et al.<sup>45</sup> found that form III was produced when high supersaturations were exposed to magnetic stirring. This result reinforces the

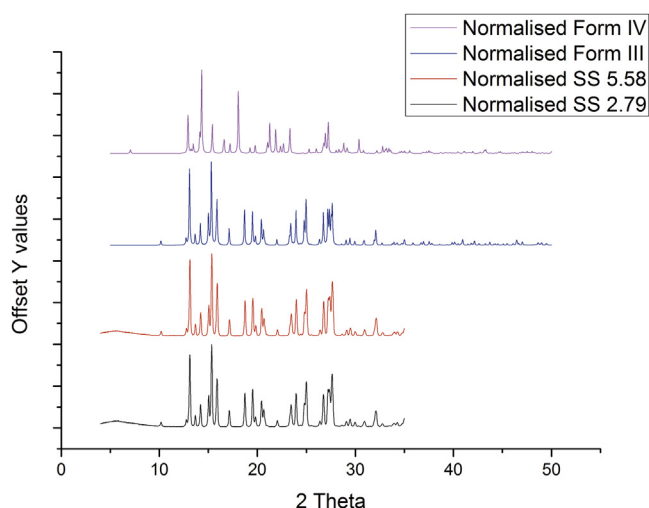


**Figure 7.** XRPD patterns of varying supersaturations in rapidly cooled methanolic CBZ solutions.

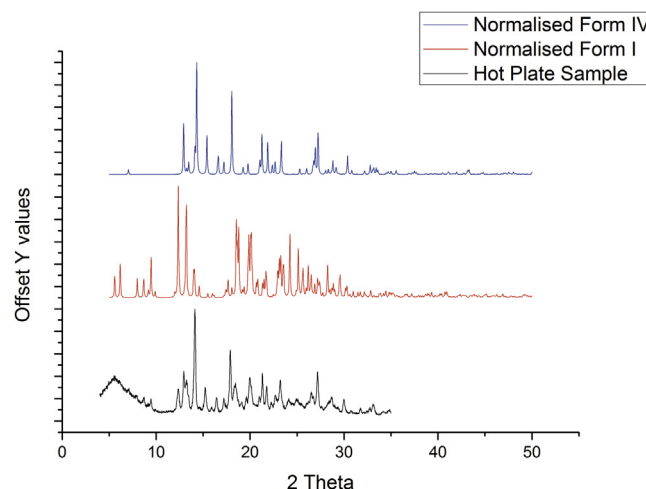


**Figure 8.** XRPD of hot plate spray-dried CBZ samples.

difficulty in obtaining CBZ IV from solution crystallization. This may be due, however, to a rapid transformation of the initial nucleated form to the stable CBZ III. To more closely mimic the conditions within a spray dryer, CBZ methanol solutions were exposed to a combination of rapid evaporation and solution isolation environments by spraying solutions onto a heated glass pane. A single glass pane was heated to 393.15 K using a hot plate, with continuous spray of CBZ methanol solution introduced to the glass surface. A suitable mass of powder was achieved in <5 min requiring small volumes of the sprayed solution and immediately analyzed by XRPD (Fig. 8).

The sample produced using this rapid evaporation method comprised a mixture of CBZ IV with a minor component of form I. This confirms the formation of form IV by rapid drying of solution out with the spray dryer. The presence of a mixture of CBZ forms in the glass-sprayed sample is suspected to be due to the lack of solid removal during continuous spraying. Hence, when the initial droplets strike the glass and evaporate, the resulting form IV particles come into contact with further liquid droplets allowing the transformation to more stable forms. When a thin layer of spray-dried form IV particles was dispersed on a clean, heated glass pane at 393.15 K onto which the CBZ methanol solution was sprayed for roughly 5 min. The particles that had been sprayed with methanol solution comprised a mixture of CBZ IV, III, and I.

Therefore, the combination of rapid drying and solid isolation in the spray dryer is an effective means of producing metastable polymorphs. This highlights the utility of spray drying in the context of solid-state and polymorph screening experiments as an effective technique to form and isolate metastable forms that may not be readily obtained from solution crystallization methods.

## Conclusion

Pure CBZ IV has been obtained reproducibly from spray drying methanol solutions in a commercial spray dryer and by rapid drying of solutions on a heated plate without the need for additives. This is in contrast to standard recrystallization methods from methanol solutions that, even under high supersaturation, tend to yield more stable forms unless specific polymeric additives are used. Rapid supersaturation during evaporation of solvent in the spray dryer (<1 s) promotes the formation of metastable forms, and continuous isolation of dried particles from solution inhibits subsequent transformation to more stable forms. The calculated drying rates and times provide a quantitative

analysis of the time boundaries that govern the crystallization of metastable polymorphic forms in the spray dryer. The rapid transformation of form IV in contact with methanol solution provides an explanation for the failure for many solution recrystallization studies to obtain CBZ IV.

## Acknowledgments

The authors would like to acknowledge The Engineering and Physical Sciences Research Council (EPSRC) and the Doctoral Training Centre in Continuous Manufacturing and Crystallisation for funding this work (grant EP/K503289/1). The authors would like to acknowledge Dr. Luke Green, Malvern Instruments Limited, for carrying out and providing the Morphologi data (Fig. 5), and Mr. Gerry Johnston, Advanced Materials Research Laboratory of the University of Strathclyde, for providing the SEM analysis (Fig. 4).

## References

1. U.S. Food and Drug Administration. *Q11 Development and Manufacture of Drug Substances (Chemical Entities and Biotechnological/Biological Entities)*. Silver Spring, MD: FDA; 2011.
2. Mullin JW. *Crystallization*. 4th ed. Oxford: Elsevier Butterworth-Heinemann; 2001.
3. *Polymorphism in the Pharmaceutical Industry*. Weinheim, Germany: Wiley-VCH Verlag GmbH & Co. KGaA; 2006.
4. Price SL. Predicting crystal structures of organic compounds. *Chem Soc Rev*. 2014;43(7):2098–2111.
5. Stahly GP. Diversity in single- and multiple-component crystals. The search for and prevalence of polymorphs and cocrystals. *Cryst Growth Des*. 2007;7(6):1007–1026.
6. Koester LS, Bertuol JB, Groch KR, Bassani LV. Bioavailability of carbamazepine: beta-cyclodextrin complex in beagle dogs from hydroxypropylmethylcellulose matrix tablets. *Eur J Pharm Sci*. 2004;22(2–3):201–207.
7. Martins RM, Siqueira S, Tacon LA, Freitas FAP. Microstructured ternary solid dispersions to improve carbamazepine solubility. *Powder Technol*. 2012;215–216:156–165.
8. Patterson JE, James MB, Forster AH, Rades T. Melt extrusion and spray drying of carbamazepine and dipyrindamole with polyvinylpyrrolidone/vinyl acetate copolymers. *Drug Dev Ind Pharm*. 2008;34(1):95–106.
9. Lang M, Kampf JW, Matzger AJ. Form IV of carbamazepine. *J Pharm Sci*. 2002;91(4):1186–1190.
10. Arlin J-B, Price LS, Price SL, Florence AJ. A strategy for producing predicted polymorphs: catemeric carbamazepine form V. *Chem Commun*. 2011;47:7074–7076.
11. Harris RK, Ghi PY, Puschmann H, et al. Structural studies of the polymorphs of carbamazepine, its dihydrate, and two solvates. *Org Process Res Dev*. 2005;9:902–910.
12. Florence AJ, Johnston A, Price SL, Nowell H, Kennedy AR, Shankland N. An automated parallel crystallisation search for predicted crystal structures and packing motifs of carbamazepine. *J Pharm Sci*. 2006;95(9):1918–1930.
13. Fleischman SG, Kuduva SS, McMahon JA, et al. Crystal engineering of the composition of pharmaceutical phases: multiple-component crystalline solids involving carbamazepine. *Cryst Growth Des*. 2003;3(6):909–919.
14. Childs SL, Wood PA, Rodriguez-Hornedo N, Reddy SL, Hardcastle KI. Analysis of 50 crystal structures containing carbamazepine using the materials module of mercury CSD. *Cryst Growth Des*. 2009;9(4):1869–1888.
15. Billinge SJL, Dykhne T, Juhás P, et al. Characterisation of amorphous and nanocrystalline molecular materials by total scattering. *Cryst Eng Comm*. 2010;12(5):1366–1368.
16. Getsoian A, Lodaya RM, Blackburn AC. One-solvent polymorph screen of carbamazepine. *Int J Pharm*. 2008;348(1–2):3–9.
17. McCabe JF. Application of design of experiment (DOE) to polymorph screening and subsequent data analysis. *Cryst Eng Comm*. 2010;12(4):1110–1119.
18. Rustichelli C, Gamberini G, Verioli V, Gamberini MC, Ficarra R, Tommasini S. Solid-state study of polymorphic drugs: carbamazepine. *J Pharm Biomed Anal*. 2000;23:41–54.
19. Grzesiak AL, Lang M, Kim K, Matzger AJ. Comparison of the four anhydrous polymorphs of carbamazepine and the crystal structure of form I. *J Pharm Sci*. 2003;92(11):2260–2271.
20. Kipouros K, Kachrimanis K, Nikolakakis I, Malamataris S. Quantitative analysis of less soluble form IV in commercial carbamazepine (form III) by diffuse reflectance Fourier transform spectroscopy (DRIFTS) and lazy learning algorithm. *Anal Chim Acta*. 2005;550(1–2):191–198.
21. Kipouros K, Kachrimanis K, Nikolakakis I, Tserki V, Malamataris S. Simultaneous quantification of carbamazepine crystal forms in ternary mixtures (I, III, and IV) by diffuse reflectance FTIR spectroscopy (DRIFTS) and multivariate calibration. *J Pharm Sci*. 2006;95(11):2419–2431.
22. Cal K, Sollohub K. Spray drying technique. I: hardware and process parameters. *J Pharm Sci*. 2010;99(2):575–586.
23. Gharsallaoui A, Roudaut G, Chamin O, Voilley A, Saurel R. Applications of spray-drying in microencapsulation of food ingredients: an overview. *Food Res Int*. 2007;40(9):1107–1121.
24. Woo MW, Bhandari B. *Spray Drying for Food Powder Production, in Handbook of Food Powders Processes and Properties*. Cambridge, UK: Woodhead Publishing; 2013:29–56.
25. Vehring R. Pharmaceutical particle engineering via spray drying. *Pharm Res*. 2008;25(5):999–1022.
26. Chawla A, Taylor KMG, Newton JM, Johnson MCR. Production of spray dried salbutamol sulphate for use in dry powder aerosol formulation. *Int J Pharm*. 1994;108(3):233–240.
27. Guimaraes TF, Lanchote AD, da Costa JS, Viçosa AL, de Freitas LAP. A multivariate approach applied to quality on particle engineering of spray-dried mannitol. *Adv Powder Technol*. 2015;26(4):1094–1101.
28. Patil SP, Modi SR, Bansal AK. Generation of 1:1 carbamazepine:nicotinamide cocrystals by spray drying. *Eur J Pharm Sci*. 2014;62:251–257.
29. Florence AJ, Baumgartner B, Weston C, et al. Indexing powder patterns in physical form screening: instrumentation and data quality. *J Pharm Sci*. 2003;92(9):1930–1938.
30. Pawley GS. Unit-cell refinement from powder diffraction scans. *J Appl Crystallogr*. 1981;14(DEC):357–361.
31. Malvern Instruments Ltd. *Morphologi G3 User Manual*. Malvern, UK: Malvern Instruments Ltd; 2015.
32. Allan P, Bellamy LJ, Nordon A, Littlejohn D, Andrews J, Dallin P. In situ monitoring of powder blending by non-invasive Raman spectrometry with wide area illumination. *J Pharm Biomed Anal*. 2013;76:28–35.
33. Bruker XS. TOPAS. Madison, WI: Bruker AXS; 1999–2014. Available at: [www.bruker-axs.com](http://www.bruker-axs.com). info@bruker-axs.de. Accessed May 12, 2017.
34. Büchi Labortechnik AG. Mini Spray Dryer B-290 Technical Data Sheet. Flawil, Switzerland: Büchi Labortechnik AG; 2015.
35. Wang M, Rutledge GC, Myerson AS, Trout BL. Production and characterization of carbamazepine nanocrystals by electrospraying for continuous pharmaceutical manufacturing. *J Pharm Sci*. 2012;101(3):1178–1188.
36. O'Mahony MA, Maher A, Croker DM, Rasmuson AC, Hodnett BK. Examining solution and solid state composition for the solution-mediated polymorphic transformation of carbamazepine and piracetam. *Cryst Growth Des*. 2012;12(4):1925–1932.
37. Huang D. *Modeling of particle formation during spray drying*. Conference abstract in: *European Drying Conference—EuroDrying*. Palma, Balearic Island, Spain; 2011.
38. Wilke CR, Chang P. Correlation of diffusion coefficients in dilute solutions. *AIChE*. 1955;1(2):264–270.
39. Coulson JM, Richardson JF. *Fluid Flow, Heat Transfer and Mass Transfer*. Oxford, UK: Butterworth-Heinemann; 1996.
40. Coulson JM, Sinnott RK, Richardson JF. *Coulson & Richardson's Chemical Engineering*. Oxford, UK: Butterworth-Heinemann; 1999.
41. Vehring R, Foss WR, Lechuga-Ballesteros D. Particle formation in spray drying. *J Aerosol Sci*. 2007;38(7):728–746.
42. Kim TU, University of Colorado at Boulder. *Transport of Organic Micropollutants through Nanofiltration (NF) and Reverse Osmosis (RO) Membranes: Mechanisms, Modeling, and Applications*. Boulder, CO: University of Colorado Boulder; 2006.
43. Yaws CL. *Yaws' Handbook of Thermodynamic and Physical Properties of Chemical Compounds*. New York: McGraw-Hill; 2003.
44. O'Mahony MA, Croker DM, Rasmuson AC, Veesler S, Hodnett BK. Measuring the solubility of a quickly transforming metastable polymorph of carbamazepine. *Org Process Res Dev*. 2013;17(3):512–518.
45. Sypek K, Burns IS, Florence AJ, Sefcik J. In situ monitoring of stirring effects on polymorphic transformations during cooling crystallization of carbamazepine. *Cryst Growth Des*. 2012;12(10):4821–4828.